

EDN: GBYSKG  
УДК 519.63

## Elastoplastic Ice Model with Dynamic Damage for Simulation of Non-linear Processes During a Low-speed Impact

Evgeniya K. Guseva\*

Vasily I. Golubev†

Igor B. Petrov‡

Computational Physics Department  
Moscow Institute of Physics and Technology  
Dolgoprudny, Russian Federation

Viktor P. Epifanov§

Ishlinsky Institute for Problems in Mechanics RAS  
Moscow, Russian Federation

Received 10.09.2024, received in revised form 25.10.2024, accepted 16.12.2024

**Abstract.** Estimation of ice deformations during dynamic loading plays a primary role in understanding many processes occurring in the Arctic region. However, the problem of choosing the most suitable model is complicated due to the complex structural changes in ice that affect its behaviour. In order to reconstruct observed damage localization, the dynamic von Mises–Schleicher criterion is applied to calculate the borders of the hydrostatic core in an elastoplastic specimen. This helps to account for the change in ice strength based on the stress magnitude. In the core, under conditions of uniform compression ice may pulverize. It results in microfracturing and recrystallization of ice. Additionally, inner and surface splits are introduced using the principal stress criterion. The model is verified with the use of numerical modelling of the laboratory experiment that consists of a direct low-speed impact. The main focus of this work is to study how non-linear processes influence the dynamics of the collision. The grid-characteristic method is used to accurately reconstruct waves formation. As a result, the formation of non-linear waves was observed. It causes further fracturing during propagation through the ice. Moreover, the conducted analysis of deformation curves confirmed that numerical results agree with the experimental data.

**Keywords:** ice rheology, non-linear waves, hydrostatic core, Von Mises–Schleicher yield criterion, fractures, low-speed impact.

**Citation:** E.K. Guseva, V.I. Golubev, I.B. Petrov, V.P. Epifanov, Elastoplastic Ice Model with Dynamic Damage for Simulation of Non-linear Processes During a Low-speed Impact, J. Sib. Fed. Univ. Math. Phys., 2025, 18(2), 177–188. EDN: GBYSKG.



Study of ice mechanical behaviour under dynamic loading remains a relevant problem that becomes especially important for the solution of practical tasks in the Arctic region. However, studying ice is complicated due to its non-linear behaviour during even for small deformations. Additionally, formulation of an adequate model is challenging because ice behaviour depends on many natural and structural factors [1] such as temperature and strain rate. Viscoelastic and elastoplastic models are commonly used for mathematical modelling, and the latter one is often applied in cases with large deformations [2, 3]. However, it is still uncertain which model would work better in specific cases. Furthermore, the influence of non-linear waves generated during impact is often assumed but not usually identified. Therefore, the main aim of this work is to

---

\*guseva.ek@phystech.su <https://orcid.org/0000-0003-2194-5081>

†golubev.vi@mipt.ru <https://orcid.org/0000-0003-3113-7299>

‡petrov@mipt.ru <https://orcid.org/0000-0003-3978-9072>

§evp@ipmnet.ru <https://orcid.org/0000-0002-9196-4264>

© Siberian Federal University. All rights reserved

study the role of wave processes occurring during impact on the dynamics of ice at low collision speeds (approximately up to 7 m/s) which are common of many processes in the Arctic region. To achieve this, the grid-characteristic method is used, which proved to be effective for many dynamic processes in complex media [4, 5].

The goal of this work is to develop the most suitable ice model with the use of laboratory experiments on the low-velocity direct impact conducted at the Ishlinsky Institute for Problems in Mechanics of the Russian Academy of Sciences. One particular feature that needs to be reflected is the observed localization of destruction in the high stress zone (contact patch) and the elastic behaviour far from the impact [2, 6]. Various criteria [7] are used to identify the hydrostactic core where ice structure can change under triaxial compression, and where microfracturing and recrystallization are observed. One of the standard choices for isotropic ice that was used in the conducted experiment is the von Mises criterion. Its advantage lies in the possibility of being modified by using a function for the calculation of yield strength. The von Mises-Schleicher criterion introduces linear relationship between this parameter and stress [8]. Thus, the observed changes in ice resistance to loading during collision are taken into account.

Another significant issue is the change in ice behaviour from the ductile behaviour and brittle failure when the deformation rates increase [1]. The considered low-velocity impacts fall into the transitional zone where both phenomena can be observed. Existing successful compound models [9] often require significant computational resources and determination of many parameters. Therefore, a simpler approach is proposed in this work to account for crack formation, where cracks appear according to the principal stress criterion [10]. As a result, this work proposes an elastoplastic model with the hydrostatic core, and boundaries of the core are calculated using the von Mises-Schleicher criterion and fracturing.

## 1. Problem formulation

### 1.1. Laboratory experiment

The laboratory experiment conducted using the procedure given in [11]. The scheme of the experiment is shown in Fig. 1. Frozen from distilled water, polycrystalline ice disc 3 was placed on the hard metal stand 4 with the ability to slide freely on its surface. A hard steel spherical indenter 2 with a piezoelectric accelerometer was hung with an inextensible string above ice surface attached to the carrier 6 with the trigger 1. The second sensor was set on the rear side of the sample along the striking axis. The whole set was placed on the metal plate 5 in a cooling chamber with the constant temperature  $-10^{\circ}\text{C}$ . As a result of the measurements, oscillograph patterns were obtained as demonstrated in Fig. 1.

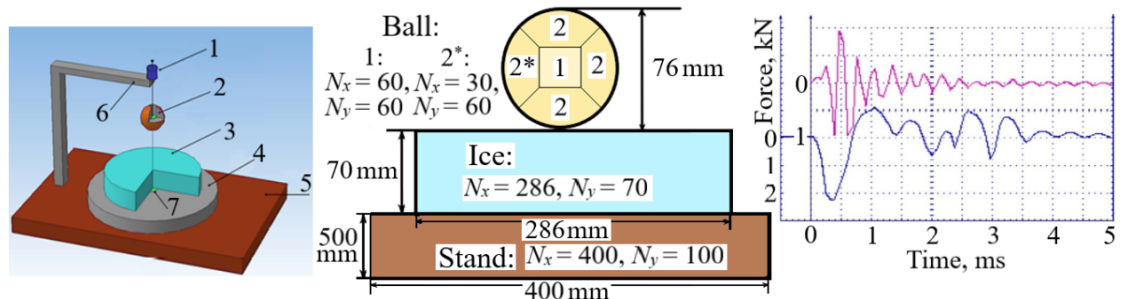


Fig. 1. On the left: the design of the laboratory experiment; in the middle: computational domain; on the right: results of the laboratory experiment (the blue line for sensor in the ball, magenta line for sensor in the ice)

## 1.2. Quantitative analysis procedure

In order to conduct quantitative comparison of the simulations and the experiment the acceleration of indenter obtained from the force  $F$  in Fig. 1 was further processed. The instantaneous velocity of the ball was obtained with integration using the Simpson rule:  $v(t) = 0.56 + \frac{1}{m} \int_0^t F(\tau) d\tau$ , with mass of the ball  $m = 1.76$  kg. However, the calculated velocity did not reach zero, presumably due to the influence of tangential velocity. To deal with this problem the transformation was conducted:  $v(t) = 0.56 \left( 1 - \frac{v - 0.56}{\min(v - 0.56)} \right)$ . Additionally, the coordinate of the ball was estimated:  $x(t) = \int_0^t v(\tau) \text{sign}(v(\tau)) d\tau$ . Here additional function  $\text{sign}(v(t))$  was introduced. It was equal to 1 during loading before velocity reaches zero and  $-1$  during unloading. Finally, in order to estimate the model deformation representing the curves positions in relation to the experiment the graph extremums were taken as the control points. They were the maximum value of the ball coordinate  $x_{\max}$  which also represents the depth of the forming dent, and the time when the velocity reaches zero  $t_{v=0}$ .

## 1.3. Computational domain

Computations were conducted in the plane setting in order to be able to thoroughly study the model qualities. Although the model evaluation in three-dimensional case is still required calculations still managed to reconstruct ice complex non-linear behaviour. The formulated computational domain in this work is presented in Fig. 1 with numbers of grid cells along the horizontal ( $N_x$ ) and the vertical ( $N_y$ ) axes. In order to construct structured grids the ball was divided into 5 parts, where domain 2 corresponds to the rotation of the domain 2\*. Full adhesion contact condition was used between areas 1–2. Free slippage condition was applied to the contact areas between the ball, the disc and the stand. Consider the dynamic ball-ice contact. If the distance between grids is less than the set value (0.05 mm) then corresponding nodes are considered to be in contact. Moreover, when normal to the surface stresses change their sign in the nodes these nodes become free. Thus, it is possible to reconstruct the effect of "glueing" and "unsticking" of the contact patch observed in the real experiments. On the left, right and bottom sides of the stand no reflection boundary was set. All other boundaries were considered to be free. Impact velocity equal to  $0.56 \frac{m}{s}$  was used as an initial condition set in the cells of the ball. All grids were moved by the Lagrange corrector. The time step equal to 25 ns was chosen to fulfil the stability condition of the calculations. The initial distance between the ball and the disc was set to be 0.05 mm. The simulations were performed until the ball stopped contacting with the ice or when the ball did not rebound from the ice.

In order to translate the set up shown in Fig. 1 into three-dimensional case for future simulations the computational domain should have rotational symmetry over the striking axis. Thus, new grids would be the surfaces of revolution of the plane grids. However, for construction of structured grids in the ice disc one needs to divide it into five parts, similarly to the grids in the ball in two-dimensional case. To keep the grid step in the impact zone equal to 1 mm as in the plain setting the number of grid nodes should be increased considerably. Ice grid in Fig. 1 has around 20 thousand nodes and if the horizontal size of the central square of the ice is set to 120–150 mm then the number of nodes can reach 1–1.6 million. The number of nodes in other four sectors can be limited to around 0.7–1 million. Therefore, the total number of nodes for the ice can equal 2.6 million which is 130-fold increase with respect to the plain grid. Similar estimations can be done for the stand and the ball. For the ball, in particular, seven grids can be constructed: one central square and six sectors. Using the numbers of grid steps that correspond to Fig. 1, the total number of nodes would increase from the initial 11 thousands to almost 1

million. Thus, during the three-dimensional modelling the number of performed operations and the real time of each calculation can increase 130-fold which would require the usage of parallel computing. Even these rough estimations incentivize the usage of the plain setting to study basic qualities of the model and its parameters.

## 2. Governing system of equations

In order to represent the ice of polycrystalline structure that was studied in the experiment the commonly used in practice isotropic linear elasticity model [12] is chosen as the governing system of equations:

$$\rho \dot{\mathbf{v}} = \nabla \cdot \boldsymbol{\sigma} + \mathbf{f}, \quad (1)$$

$$\dot{\boldsymbol{\sigma}} = \lambda(\nabla \cdot \mathbf{v})\mathbf{I} + \mu(\nabla \otimes \mathbf{v} + (\nabla \otimes \mathbf{v})^T). \quad (2)$$

Here, the unknown velocity  $\mathbf{v}$  and stress tensor  $\boldsymbol{\sigma}$  are calculated at each time step using the Lamé parameters  $\lambda$ ,  $\mu$  and density  $\rho$ . These parameters can be used to calculate speeds of pressure and shear waves:  $c_p = \sqrt{\frac{\lambda + 2\mu}{\rho}}$  and  $c_s = \sqrt{\frac{\mu}{\rho}}$ . As a result,  $c_p$ ,  $c_s$  and  $\rho$  fully define the behaviour of system (1)–(2). External volumetric forces can be introduced with  $\mathbf{f}$ . For the simulations, the material parameters for hard steel are used for the ball and the metal stand:  $c_p = 5700 \frac{m}{s}$ ,  $c_s = 3100 \frac{m}{s}$ ,  $\rho = 7800 \frac{kg}{m^3}$ . Ice parameters were estimated using the Berdennicov formula ( $E = (87.6 - 0.21T - 0.0017T^2) \cdot 10^8$  Pa, [13]) with the same temperature as in the laboratory experiment and the constant Poisson coefficient  $\nu = 0.295$ . Then parameters for ice are  $c_p = 3600 \frac{m}{s}$ ,  $c_s = 1942 \frac{m}{s}$ ,  $\rho = 917 \frac{kg}{m^3}$ .

## 3. Computational method and scheme

Nowadays, there is no standard method to solve ice problems related to dynamic loading [14]. Although the finite element methods [15], coupling methods [16] and various mesh-free methods such as peridynamics [17] are gaining popularity. However, a lot of them still have disadvantages. They are mainly related to the representation of fracturing. As the focal point of this work is the study of wave phenomena linked to the occurring damage the grid-characteristic method was chosen to solve equations (1)–(2). This method allows one to accurately reproduce dynamic processes as proven in [4, 5]. The method uses the hyperbolicity of system (1)–(2) in order to conduct coordinate-wise and process-wise splitting and change of the variables to the Riemann invariants. As a result, the initial system can be reduced to a system of independent one-dimensional transport equations. In this case, each equation is solved using the third approximation order grid-characteristic scheme monotonized by the grid-characteristic monotonicity criterion [18].

## 4. Nonlinear rheological models

Splitting on physical processes allows one to take into account non-linear behaviour. All such models modify the elastic solution after each calculation step. The introduced compound model consists of the elastoplastic ice with the hydrostatic core and fractures.

### 4.1. Elastoplasticity model

Plasticity is described as the Prandtl–Reuss flow rule [19] that corrects the stress deviator ( $s_{ij}^{el} = \sigma_{ij}^{el} - \frac{\sigma_{ll}^{el}}{\delta_{mm}} \delta_{ij}$ ) to return the stress tensor to the von Mises yield surface (if  $\frac{1}{2} s_{ij}^{el} s_{ij}^{el} - k^2 > 0$ ):

$$s_{ij} = s_{ij}^{el} \frac{\sqrt{2}k}{\sqrt{s_{pq}^{el} s_{pq}^{el}}},$$

The defining parameter of the model is the maximum shear stress  $k$ . The initial state of the ice is considered to be elastoplastic. During the collision, calculated elastic variables are used to check the fulfilment of criteria for formation of the hydrostatic core at each time step. Then, the elastoplasticity in the ice is realized outside of the core.

## 4.2. Hydrostatic core

In order to account for structural changes in ice the approach formulated in [10] is used. The damage is divided into static and dynamic part. The static damage is represented as the formation of the hydrostatic core. It is a zone where the ice is under the triaxial compression due to loading of the ball. Here complex structural changes such as microfracturing and recrystallization can occur. Boundaries of this zone are defined on the basis of the von Mises-Schleicher criterion. It is a modified version of the von Mises criterion that allows for taking into account the change in the ice strength during collision. This is realized as follows. The constant shear stress value is replaced with a linear function  $k_0 + ap$ , where  $p = \frac{\sigma_{ll}}{\delta_{mm}}$  is the instantaneous value of pressure in the node. In order to represent material inside the core the sand model [10] is used. It considers that damaged material could not sustain tension. Thus, all positive principal stresses are set to zero. Moreover, instead of elastoplastic stress tensor correction elastic parameters are changed, and the Lamé parameter  $\mu$  is decreased by a factor of 100 to represent the almost liquid state of the ice.

## 4.3. Fracture model

The dynamic damage is described by taking fracturing into account [10]. If the principal stresses exceeded the spallation strength  $k_s$  in some node of the ice disc grid then a unit fracture is formed. The size of the fracture is not defined within the cell, and it is considered to be less than spacial step. As a result, the growth of cracks is described as the increase in the number of such unit fractures. Free boundary conditions are used in each damaged node in order to reconstruct the observed reflections from fractures. This allows for the reconstruction of time-dependent behaviour of ice by observing the complex interactions between wave and damage processes.

## 4.4. The compound model algorithm

To sum up the process of the model implementation the following procedure is conducted at each time step of simulations. At first, the elastic values of unknown variables  $\mathbf{v}^{el}$  and  $\sigma^{el}$  are calculated and corresponding coordinate-wise splitting boundary and interface conditions are implemented. Then, the von Mises-Schleicher criterion is used to determine the boundaries of the core. If condition  $\frac{1}{2}s_{ij}^{el}s_{ij}^{el} - (k_0 + ap)^2 > 0$  is fulfilled then correction of principal stresses and elastic parameters is performed in each grid node of the ice in accordance with the core model. In the nodes outside the core stress tensor deviator is corrected when the von Mises criterion  $\frac{1}{2}s_{ij}^{el}s_{ij}^{el} - k^2 > 0$  is satisfied as the elastoplastic model suggests. Finally, the principal stress condition for fracturing is checked in each node, and fractures appear in corresponding nodes. After all corrections are performed grids are moved.

## 5. Simulation results

As a result of simulations, wave, stress and damage patterns (Figs. 2–4) are obtained and used for the comparison with the experiment. Moreover, graphs of the ball velocity and coordinate

are used for quantitative evaluations (Figs. 5–6).

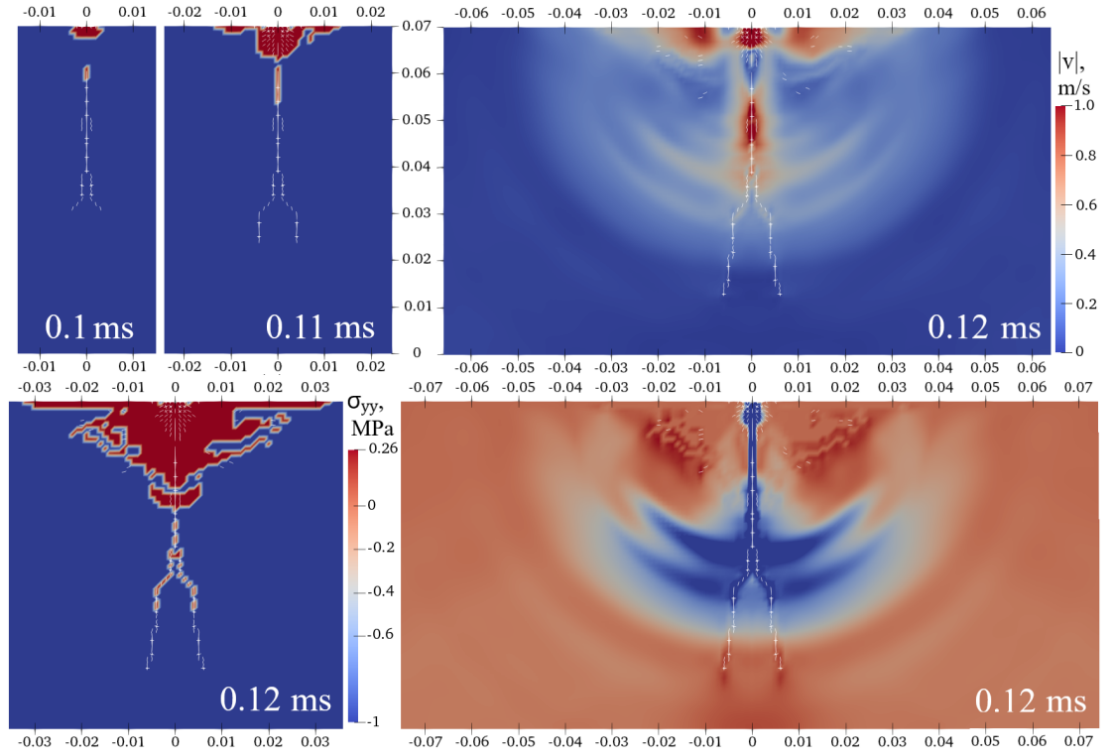


Fig. 2. Left column: damage patterns, core (red) and fractures (white). Right column: nonlinear wave ( $|v|$ ) and stress (vertical stress projection  $\sigma_{yy}$ ) patterns. Coordinates are in meters,  $k = k_0 = k_s = 0.3$  MPa,  $a = 0.1$

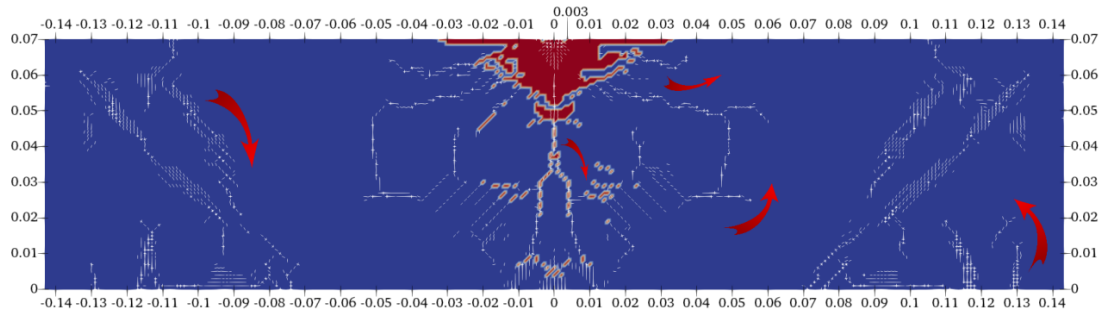


Fig. 3. Damage patterns, core (red) and fractures (white) at 0.23 ms,  $k = k_0 = k_s = 0.3$  MPa,  $a = 0.1$ . Arrows show the direction of fracture growth. Radius of the contact patch is 3 mm. Coordinates are in meters

### 5.1. Qualitative comparison with the experiment

Simulations show that behaviour of the model can be drastically changed with different damage parameters. For big values of  $k_0$  and  $k_s$  damage (core and fractures) is usually localized near the impact zone (similar to patterns at 0.1 ms in Fig. 2). At the initial stages of collision,

the first cracks start to appear in the area with the biggest stress on the contact patch. Vertical cracks form near the boundary of the patch, and their number increases as this boundary moves along with the ball indentation. Moreover, the core forms directly under the surface fractures. Its size usually corresponds to the diameter of the contact. Similar localization of fracture can be observed in real experiments [20, 21]. Additionally, a median fracture can be formed with the propagation of the impact wave. Its growth starts at a distance from the contact, and it is additionally stimulated by the reflected wave. Sometimes this crack can be split into two parts, forming an arch similar to Fig. 2 at 0.12 ms. However, further inner spalling does not occur.

When  $k_s$  is decreased, the principal stress criterion starts to be fulfilled in a greater number of nodes, and fracture begin to spread through the disc. As shown in Fig. 2, at certain points of time the number of cracks can increase exponentially starting from the impact zone. This phenomenon is seemingly caused by interference between the reflected impact waves and waves generated from the contact patch due to the surface fracture and waves that propagate in the ball. The rapid growth of fractures invokes non-linear waves that create further damage far from the impact zone. With the forward travel of the wave fractures grow from the core, and side cracks can appear. After reflection cracks begin to form from the rear surface. The damage patterns are fully developed by the time of the unloading as in Fig. 3.

A similar phenomenon can be observed when the value of  $k_0$  is small and the fractures are localized or not taken into account completely as in Fig. 4. This case clearly demonstrates the influence of  $a$  on the results. When  $a = 0$ , the core usually has homogeneous structure and not many discontinuities. On the contrary, non-zero  $a$  can change the form of the core, and it begins to resemble fractures (Fig. 4). However, when  $a$  is too big, the von Mises–Schleicher criterion is rarely satisfied and the core is localized at the impact zone. When  $a < 1$ , the centre of the core is usually formed in the nearest neighbourhood of the contact patch. The rapid increase in the core area can also generate non-linear waves that cause patterns similar to conical (middle picture) and side (top and middle pictures) cracks and horizontally oriented clusters of fractures (bottom picture). Additionally, the spread of the core zones starting from the rear surface of the ice can also be recreated (bottom picture). As a result, the appearance of non-linear waves represents a distinct interaction between the wave and damage processes that was usually assumed but not clearly demonstrated in previous works.

## 5.2. Quantitative comparison with the experiment

The influence of model parameters on wave patterns and fracture patterns is studied on the basis of deformation curves in Fig. 5. The velocities obtained from the laboratory experiment can be divided into three stages: the inlet section (up to about 0.2 ms), the main stage of impact (from 0.2 to 0.6 ms) and the time near the rebound (from 0.6 to 0.8 ms). The gradual decrease of the velocity during the first and last stages may be related to the temperature effects and surface tension that influence the formation of the dent and the hardening processes. The inlet section was not reconstructed during the simulation. However, it is in the case of small values of  $k_0$  when it is possible to qualitatively represent the experiment by the time of unloading. This is demonstrated by similar slopes of the calculated and experimental curves and tapering of the velocity.

Moreover, Fig. 5 shows the distinction in behaviour between the small and big values of  $k_0$ . Small value of  $k_0$  leads to a larger core, higher amplitudes of coordinates, less monotone velocity, and bigger times when the velocity reaches minimum. This trend appears both with (second row) and without (first row) fractures. Thus, it is possible to find the optimal parameters of the model to reach agreement with the experiment. As a result, the closest to the experiment curve is in the case without fractures:  $k = 0.03$  MPa,  $k_0 = 0.08$  MPa,  $a = 0.5$ . However, when the value of  $k_0$  is big the von Mises–Schleicher criterion stops to be satisfied, and the curves for various  $a$  almost coincide.

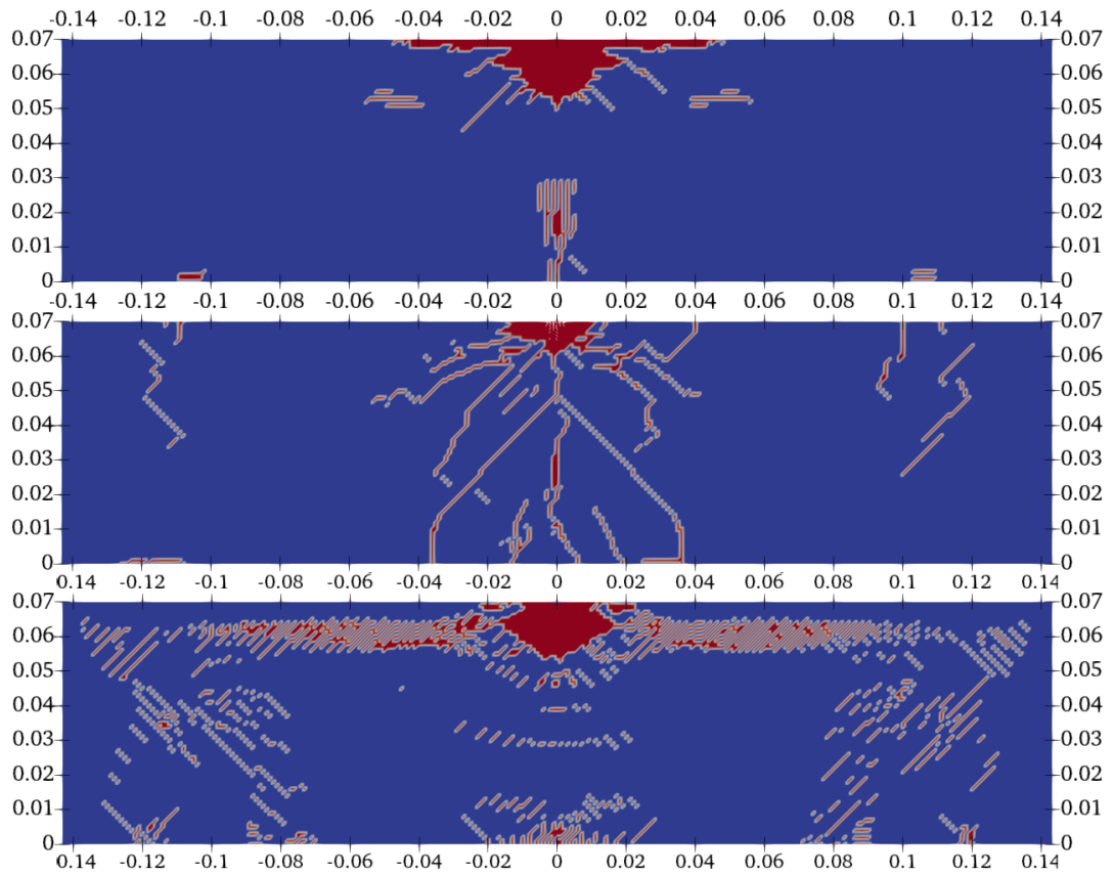


Fig. 4. Damage patterns: core (red) and fractures (white). Picture at the top: no fractures,  $k = 0.08$  MPa,  $k_0 = 0.1$  MPa,  $a = 0.1$ , 0.4 ms. Picture at the top middle: with fractures,  $k = 0.08$  MPa,  $k_0 = 0.1$  MPa,  $k_s = 0.3$  MPa,  $a = 0.5$ , 0.9125 ms. Picture at the bottom: no fractures,  $k = 0.3$  MPa,  $k_0 = 0.08$  MPa,  $a = 0.5$ , 0.3 ms

Similar trends can be observed when  $a$  and  $k$  are varied. However, the introduction of  $a$  generally results in significant oscillations and less monotonous graphs of velocity. Nonetheless, the change in  $a$  allows for the achievement of the optimal parameters of the model as shown in Fig. 6 for small enough values of  $k_0$ . These parameters can be predicted using the intersection between numerical results with the experimental values of  $x_{\max}$  and  $t_{v=0}$ . Therefore, this allows for the usage of optimization algorithms and machine learning to train the model. Furthermore, this approach can be used for both variations of the model with and without fractures. As it is shown in Fig. 5 (third row), the calculated curves are very similar, especially for small values of  $a$ . However, the influence of the spallation strength  $k_s$  is ambiguous. Thus, a more thorough evaluation is still required. As a result, the model proved to be able to reconstruct many aspects of ice behaviour during the impacts. Although the deformation curves do not coincide completely with the experimental ones, the simulations represent the experiment during the main stage of the collision. Moreover, the model allows for the optimization of its parameters. It is one of the main directions for further work.



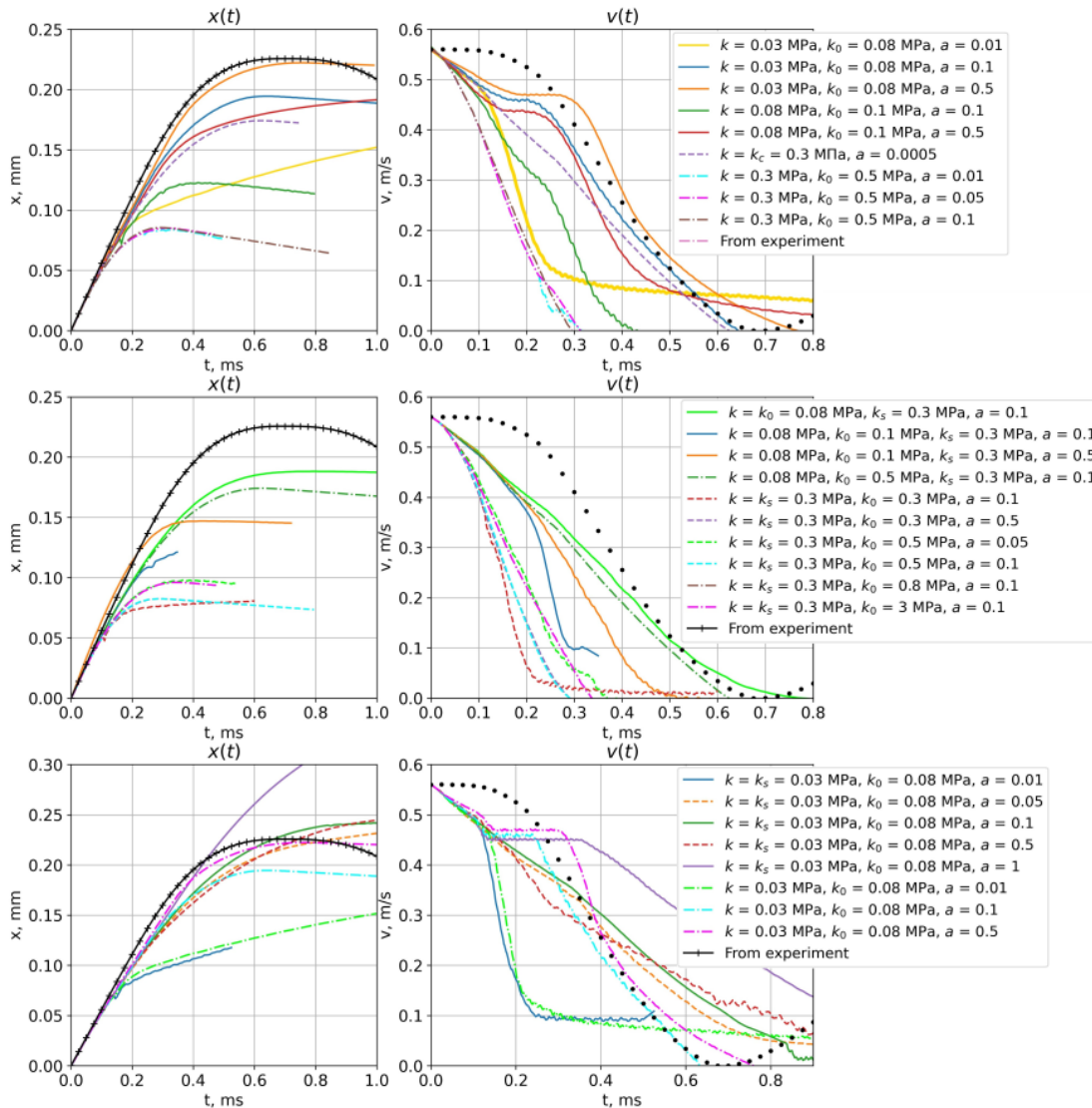


Fig. 5. Ball coordinate ( $x$ ) and velocity ( $v$ ) during the collision for various parameters of the model. First row – no fractures, second row – with fractures, third – comparison of the cases with and without fractures

## Conclusion

As a result of this work, the compound model is used to describe ice behaviour during a low-speed impact by a spherical indenter. The observed localization of damage and the change in ice local resistance to loading are accounted for by the determination of the hydrostatic core in the elastoplastic sample using the dynamic von Mises–Schleicher yield criterion. Fracturing is introduced using the maximum principle stress criterion. Thus, it is possible to reconstruct ice complex and time-dependent behaviour with the obtained formation of non-linear waves that cause further damage. Moreover, both core and fractures could represent different types of cracks, such as median, side and conical fractures. The cracks formed on the contact patch from the rear surface and far from the impact zone. The qualitative analysis of deformation curves proves

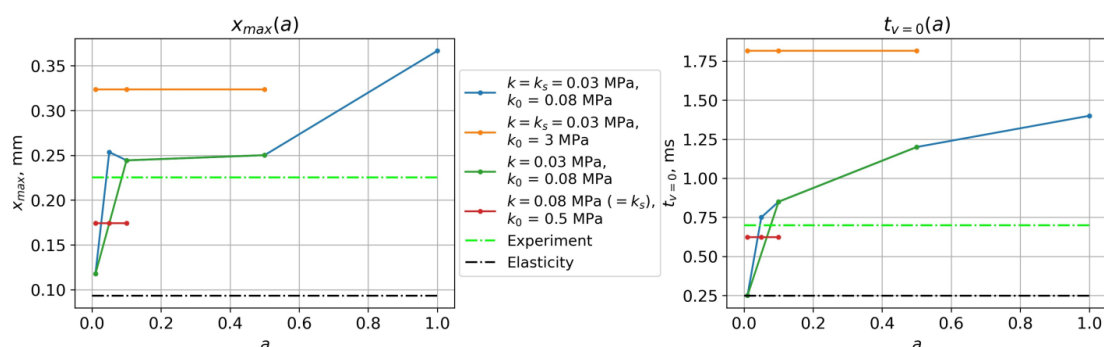


Fig. 6. Maximum ball coordinate and velocity in relation to parameter  $a$ . For reference, the values obtained with the use of standard elasticity model for ice are marked by black line

the ability of the model to reach an agreement with the experiment. Therefore, a more detailed optimization of parameters of the model both in a plane and space setting is the main direction for further work.

*The reported study was carried out with the financial support of the Russian Science Foundation, project no. 23-21-00384.*

## References

- [1] S.T.Ince, A.Kumar, J.K.Paik, A new constitutive equation on ice materials, *Ships Offshore Struct.*, **12**(2017a), no. 5, 610–623. DOI: 10.1080/17445302.2016.1190122
- [2] I.Jordaan, Some issues in ice mechanics, *Proceedings of the ASME 2015 34th International Conference on Ocean, Offshore and Arctic Engineering*, **8**(2015), OMAE2015-42042. DOI: 10.1115/OMAE2015-42042
- [3] M.Mokhtari, B.J.Leira, A critical review of constitutive models applied to Ice-Crushing simulations, *Journal of Marine Science and Engineering*, **12**(2024), no. 6, 1021. DOI: 10.3390/jmse12061021
- [4] A.V.Favorskaya, I.B.Petrov, Calculation of seismic stability of buildings in the Far North using the Grid-Characteristic Method, *Lobachevskii Journal of Mathematics*, **45**(2024b), no. 1, 213–222. DOI: 10.1134/S1995080224010153
- [5] N.I.Khokhlov, I.B.Petrov, Application of the grid-characteristic method for solving the problems of the propagation of dynamic wave disturbances in high-performance computing systems, *Proceedings of the Institute for System Programming of RAS*, **31**(2019), no. 6, 237–252. DOI: 10.15514/ISPRAS-2019-31(6)-16
- [6] P.Barrette, J.Pond, I.Jordaan, Ice damage and layer formation in small-scale indentation experiments, *Ice in the Environment: Proceedings of the 16th International Association for Hydraulic Engineering and Research (IAHR) International Symposium on Ice, 2002*, 246–253.
- [7] W.Zhang, J.Li, L.Li, Q.Yang, A systematic literature survey of the yield or failure criteria used for ice material, *Ocean Engineering*, **254**(2022), 111360. DOI: 10.1016/j.oceaneng.2022.111360

- 
- [8] A.M.Kovrizhnykh, Plane Stress Equations for the Von Mises-Schleicher Yield Criterion, *Journal of Applied Mechanics and Technical Physics*, **45**(2004), 894–901. DOI: 10.1023/B:JAMT.0000046039.92532.fd
- [9] M.Mokhtari, E.Kim, J.Amdahl, A non-linear viscoelastic material model with progressive damage based on microstructural evolution and phase transition in polycrystalline ice for design against ice impact, *International Journal of Impact Engineering*, **176**(2023b), 104563. DOI: 10.1016/j.ijimpeng.2023.104563
- [10] A.Favorskaya, V.Golubev, D.Grigorievyh, Explanation the difference in destructed areas simulated using various failure criteria by the wave dynamics analysis, *Procedia Computer Science*, **126**(2018), 1091–1099. DOI: 10.1016/j.procs.2018.08.046
- [11] V.P.Epifanov, Ice destruction from impact interactions, *Akademiia Nauk SSSR Doklady*, **284**(1985), no. 3, 599–603. DOI: 10.1007/978-3-031-54589-4\_29
- [12] V.Novatskii, Theory of Elasticity, Mir, Moscow, 1975 (in Russian).
- [13] V.P.Berdennikov, Izuchenie modulya uprugosti lda, *Trudi GGI*, **7**(1948), no. 61, 13–23 (in Russian).
- [14] D.Grinevich, V.Buznik, G.Nuzhnyi, Review of numerical methods for simulation of the ice deformation and fracture, *Proceedings of VIAM*, **8**(2020), 109–122 (in Russian). DOI: 10.18577/2307-6046-2020-0-8-109-122
- [15] H.Jang, S.Hwang, J.Yoon, J.H.Lee, Numerical analysis of Ice-Structure impact: Validating material models and yield criteria for prediction of impact pressure, *Journal of Marine Science and Engineering*, **12**(2024), no. 2, 229. DOI: 10.3390/jmse12020229
- [16] R.Sun, Z.Li, Y.Shi, Numerical simulation of ice loading characteristics of ships in a wave-current environment in a broken ice area, *Journal of Physics Conference Series*, **2756**(2024), no. 1, 012030.
- [17] Y.Song, L.Zhang, S.Li, Y.Li, A Multi-Yield-Surface Plasticity State-Based Peridynamics Model and its Applications to Simulations of Ice-Structure Interactions, *Journal of Marine Science and Application*, **22**(2023), no. 3, 395–410. DOI: 10.1007/s11804-023-00344-8
- [18] E.K.Guseva, V.I.Golubev, I.B.Petrov, Linear, Quasi-Monotonic and Hybrid Grid-Characteristic Schemes for Hyperbolic Equations, *Lobachevskii J. Math.*, **44**(2023), 296–312. DOI: 10.1134/S1995080223010146
- [19] O.T Bruhns, The Prandtl-Reuss equations revisited, *Z. Angew. Math. Mech.*, **94**(2014), no. 3, 187–202.
- [20] V.P.Epifanov, Physical mechanisms of ice contact fracture, *Dokl. Phys.*, **52**(2007), no. 1, 19–23. DOI: 10.1134/S1028335807010053
- [21] V.P.Epifanov, Contact fracture behavior of ice, *Ice and Snow.*, **60**(2020), no. 2, 274–284 (in Russian). DOI: 10.31857/S2076673420020040

## Упругопластическая модель льда с динамическим разрушением для моделирования нелинейных процессов во время низкоскоростного удара

Евгения К. Гусева

Василий И. Голубев

Игорь Б. Петров

Кафедра вычислительной физики

Московский физико-технический институт

Долгопрудный, Российская Федерация

Виктор П. Епифанов

Институт проблем механики им. Ишлинского РАН

Москва, Российская Федерация

**Аннотация.** Определение деформации льда в процессе приложения динамических нагрузок играет первостепенную роль для понимания многих процессов, происходящих в Арктическом регионе. Однако решение задачи выбора наиболее подходящей модели усложняется из-за происходящих структурных изменений, влияющих на поведение льда. Для отражения наблюдаемой локализации разрушений применяется динамический критерий Мизеса–Шлейхера для выделения гидростатического ядра в упругопластическом образце льда. Таким образом, также учитывается изменение прочности льда в зависимости от величины напряжений. В ядре в условиях всестороннего сжатия лед может крошиться, возможно образование микротрещин и рекристаллизация. Дополнительно учитывается трещинообразование в объеме материала с помощью критерия по главным напряжениям. Модель верифицируется на основе моделирования лабораторного эксперимента по низкоскоростному прямому удару. Основной особенностью данной работы является изучение влияния нелинейных процессов на динамику столкновения. Применение сеточно-характеристического метода позволяет точно разрешать образующиеся волны. В результате удалось продемонстрировать образование нелинейной волны, вызывающей трещинообразование при прохождении через лед. К тому же, анализ деформационных кривых подтвердил возможность согласования расчетов с экспериментом.

**Ключевые слова:** реология льда, нелинейные волны, критерий текучести Мизеса–Шлейхера, трещины, низкоскоростной удар.